Carbohydrate Polymers 88 (2012) 321–328

Contents lists available at SciVerse ScienceDirect

Carbohydrate Polymers

journal homepage: www.elsevier.com/locate/carbpol

Effects of clays with various hydrophilicities on properties of starch–clay nanocomposites by film blowing

Wei Gao, Haizhou Dong, Hanxue Hou*, Hui Zhang

Department of Food Science and Engineering, Shandong Agricultural University, Tai'an 271018, PR China

ARTICLE INFO

Article history:
Received 23 September 2011
Received in revised form
29 November 2011
Accepted 11 December 2011
Available online 19 December 2011

Keywords:
Clays
Hydrophilicity
Extrusion blowing
Nanocomposite film
Physical and mechanical properties
Hydroxypropyl distarch phosphate

ABSTRACT

Effects of clays with various hydrophilicities on the physical and mechanical properties of hydroxypropyl distarch phosphate–nanoclay composite films by extrusion blowing were investigated. Five kinds of organically modified clays with different hydrophilic properties were used in the preparation of starch nanocomposite films. X-ray diffraction (XRD) and transmission electron microscopy (TEM) showed the formation of intercalated nanostructure to a certain extent. With the addition of clays, significantly greater tensile strength (TS, 2.51 MPa) and lower water vapor permeability (WVP, 3.69×10^{-10} g m/(m^2 s Pa)) were obtained. Starch–clay composite films exhibited a lower glass transition temperature (T_g, −23.8 °C) and better heat endurance with differential scanning calorimetry (DSC). The addition of clays to starch had a negative effect on the interaction between starch and plasticizer by FTIR spectra. Organically modified clays were helpful in the melting and fracturing of starch granules in the extrusion revealed by a scanning electronic microscope (SEM). The clay with medium hydrophilic property was more suitable for the production of hydroxypropyl distarch phosphate–clay nanocomposite films as an intensifier among the five clays.

1. Introduction

The applications of disposable petrochemical-based plastic materials are increasing significantly and have led to serious ecological problems because they are totally non-biodegradable. In recent years there have been greater efforts to develop new biodegradable materials from natural and renewable resources which can result in easily tailored composite materials (Medeiros, Dufresne, & Orts, 2010). Although it is impossible to achieve complete replacement by eco-friendly packaging materials, at least for some specific applications like food packaging, the use of bioplastics should be a trend (Siracusa, Rocculi, Romani, & Rosa, 2008).

Starch has received considerable attention and has been considered as one of the most promising candidates for the production of biodegradable materials because of its easy availability, relatively low cost, and renewable natural polysaccharide obtained from a great variety of crops (Kalambur & Rizvi, 2004; Lopez, Garcıa, & Zaritzky, 2008; Thunwall, Kuthanova, Boldizar, & Rigdahl, 2008; Zullo & Iannace, 2009). However, the use of starch-based films for food packaging has been very limited because of their poor stability in processing (such as low heat depolymerization temperature), weak mechanical properties, poor moisture barrier and high sensitivity to the environmental changes such as humidity, temperature, and PH (Azeredo, 2009; Chung et al., 2010). These drawbacks have to be overcome to obtain better performance of starch-based biomaterials.

Several attempts were made to improve starch-based materials by adding reinforced compounds, resulting in materials with moderately improved properties, but with limited processability and poor compatibility due to high viscosity and interfacial energy (Guan, Eskridge, & Hanna, 2005; Medeiros et al., 2010; Sarazin, Li, Orts, & Favis, 2008; Sita, Burns, Haßler, & Focke, 2006). Recently, starch-based nanocomposites with the addition of low quantities of fillers have given rise to significant improvements in physical, mechanical, and barrier properties (Wilhelm, Sierakowski, Souza, & Wypych, 2003a; Wilhelm, Sierakowski, Souza, & Wypych, 2003b). Layered silicates (clays) have become one of the most popular nanomaterials in the research of biodegradable food packaging materials due to their availability, low cost, significant enhancements and relative simple processability.

Carvalho, Curvelo, and Agnelli (2001) first investigated the preparation and characterization of thermoplasticized starch–kaolin composites by melt intercalation techniques. After that, several researches have been conducted on the preparation of starch/clay nanocomposites by melt intercalation (Avella et al., 2005; Chen & Evans, 2005; Chiou et al., 2007; Huang, Yu, & Ma, 2006; Kalambur & Rizvi, 2004; Qiao, Jiang, & Sun, 2005; Tang, Alavi, & Herald, 2008). The various properties of starch/clay

* Corresponding author. Tel.: +86 538 824 5855; fax: +86 538 8242850.
E-mail addresses: houhanxue@yahoo.com.cn, hhx@sdau.edu.cn (H. Hou).

0144-8617/$ – see front matter © 2011 Elsevier Ltd. All rights reserved.
doi:10.1016/j.carbpol.2011.12.011

nanocomposites were greatly influenced by silicate functionalization and starch molecular structure which determined the degree of penetration of the starch chains into the silicate galleries. The natural smectite clays easily formed nanocomposites with native starches while organically modified smectite formed conventional composites with native starches (Chen & Evans, 2005; Park et al., 2002; Tang et al., 2008). However, organically modified montmorillonite (OMMT) tended to form complete intercalation structure of nanocomposites with some types of modified starches (Qiao et al., 2005). The compatibility and the polar interaction between modified starches and OMMT should be further studied.

Extrusion film blowing is a continuous, energy-efficient process with high productivity of biodegradable films (Thunwall et al., 2008). However, up to date, there have been very few reports on starch-based nanocomposite films by extrusion blowing. In this study, effects of organically modified montmorillonites with different hydrophilicities on physical and mechanical properties of hydroxypropyl distarch phosphate–clay nanocomposite films by extrusion blowing were investigated.

2. Materials and methods

2.1. Materials

Five types of nanoclays (Cloisite Na^+) which were modified by different quaternary ammonium salts were provided by Zhejiang Fenghong Co. Ltd (Zhejiang, China). The surface hydrophilic property of the clays was in the order of DK5 > DK2 > DK3 > DK1 > DK4. Hydroxypropyl distarch phosphate (HPDSP) was purchased from Puluoxing Starch Co. Ltd (Hangzhou, China). Glycerol was obtained from Chemical Reagent Co. Ltd (Tianjin, China).

2.2. Preparation of the starch–nanoclay composite films

Starch, glycerol (35% in relation to starch mass), clay (6% in relation to starch mass) were thoroughly blended in a SHR50A mixer (Hongji Co., Ltd., Zhangjiagang, China) at room temperature for 10 min. Blended mixtures were stored in polyethylene bags at room temperature overnight to equilibrate all components. Extrusions of the blends were done in a laboratory-scale twin screw extruder (Jingrui Plastic Machinery Co., Ltd., Laiwu, China). Temperatures of extrusion were at 80 °C and 125 °C in I and II zones of the barrel, respectively. The mixtures were extruded at a screw speed of 30 rpm. The extrudates were cut into pellets and conditioned for at least 72 h prior to film blowing at 53% relative humidity and 23 °C.

Film blowing was performed using a single screw extruder (Jingrui Plastic Machinery Co., Ltd., Laiwu, China), with a screw diameter of 35 mm, screw length of 25D and four individually controlled temperature zones. A screw with a compression ratio of 3:1 was used in this study. The extruder was equipped with a conventional temperature-controlled film-blowing die with a diameter of 60 mm and a film-blowing tower with a calendaring nip and take-off rolls. Temperatures in the barrel and die were maintained at 80 °C, 120 °C, 130 °C, 140 °C and 135 °C from feed inlet to die, respectively. The contrast film was prepared under the same conditions without clay. Fig. 1 showed the continuous and stable preparation of starch–nanoclay composite films by film blowing.

2.3. Mechanical properties

Mechanical properties of the films were determined by tension tests, with a TA-XT2i texture analyzer (Stable Micro System Company, UK) according to ASTM-D882-02 (2002). All of the tested films, equilibrated at 23 ± 2 °C and 53% relative humidity ($Mg(NO_3)_2$ saturated solution) for at least 72 h prior to testing, were cut into strips (15 mm × 100 mm) with a sharp knife. The testing environment was also 53% relative humidity and 23 ± 2 °C. The initial distance between the grips is 50 mm. The test speed is 1 mm/s. Tensile strength (TS, MPa) and elongation at break (E, %) were calculated by six replicates based on previous reports (Tang et al., 2008).

2.4. Water vapor permeability

Water vapor permeability (WVP) was determined with a PERME^{TM}W3/030 water vapor permeability tester (Labthink Instruments CO. Ltd, China). Films were cut into round shape (80 mm in diameter) with a special sampler. The specimens should remain smooth and have no wear, wrinkle and breakage, and was placed in the condition of 23 ± 2 °C and 50 ± 5% RH for at least 48 h according to GB1037-88. Test parameters were set at preheating time of 4 h, test judgment of 10%, test temperature at 38.0 °C, test humidity of 90% RH and weighing interval of 120 min. Water vapor permeability of each sample was averaged from three separate tests.

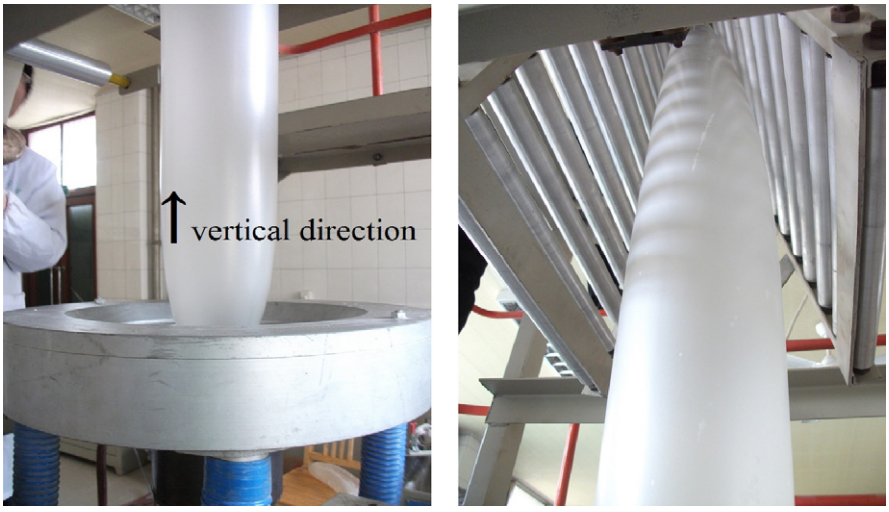

Fig. 1. Continuous and stable film blowing of starch–nanoclay composites.

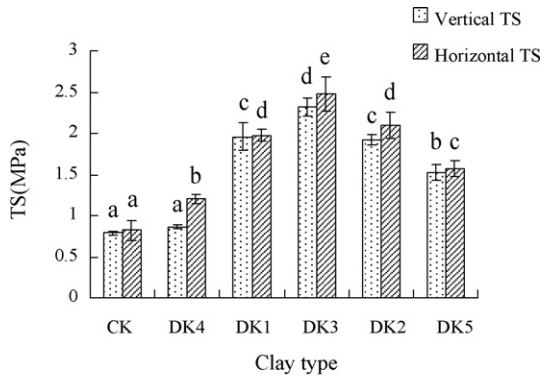

a. Vertical and horizontal tensile strength of starch- nanoclay composite film

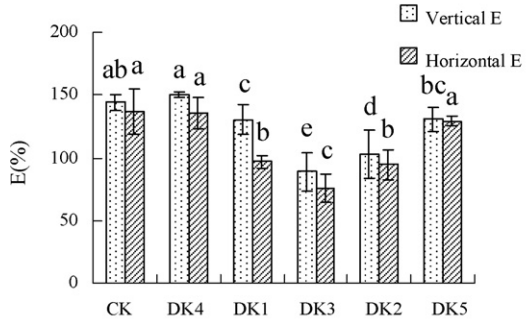

b. Vertical and horizontal Elongation at break of starch- nanoclay composite films

Fig. 2. Mechanical property of starch–nanoclay composite films (TS – tensile strength; *E* – elongation at break; CK – blank control).

2.5. Differential scanning calorimetry

The glass transition temperature (T_g) and transition temperatures (onset temperature, T_o and peak temperature, T_p) of various starch–clay nanocomposite films were determined with a DSC 200PC (NETZSCH Scientific Instruments, Germany). Samples of the films were first equilibrated at 23 °C and 50% RH for more than two days. Then samples of 5–10 mg were weighed in aluminium pans and hermetically sealed. An empty, hermetically sealed aluminium pan was used as the reference. The heating rate was 10 °C/min with a heating cycle from −70 °C to 260 °C. Liquid nitrogen was used for the running of all scans. Each sample was tested three times. The testing environment was also 53% relative humidity and 23 ± 2 °C.

2.6. X-ray diffraction and transmission electron microscopy

X-ray diffraction (XRD) properties of the films were carried out with a D8 Advance X-ray diffractometer (Bruker-AXS, Germany). Samples were scanned in the range of diffraction angle $2\theta = 1–10^\circ$ at a step of 0.02° and step time of 1 sec. The basal spacing of the silicate layer (d_{001}) was calculated using Bragg's diffraction equation, $\lambda = 2d \sin\theta$, where λ is the wavelength of the X-ray radiation used (0.15406 nm), d is the spacing between diffraction lattice planes and θ is the measured diffraction angle.

Transmission electron microscopy (TEM) was performed with a Tecnai 20U-TWIN electron microscope (Philips, the Netherlands) operating at 100 kV. Ultra-fine grinding samples were placed onto a carbon-coated copper grid by physically interacting the grid and powders and were analyzed to see the dispersion of layers.

2.7. FTIR analysis

The Fourier transform infrared (FT-IR) spectra of the films were measured in a Thermo Fisher Scientific (USA) Nexus 670 spectrometer attached to the Smart iTR diamond ATR accessory in the wavelength range of 600–4000 cm^{-1}. The resolution was 4 cm^{-1}. The number of accumulated scans was 32. The film was mounted directly in the sample holder (Sudhamani, Prasad, & Udaya Sankar, 2003).

2.8. Scanning electronic microscope (SEM)

Scanning electron microscopy (SEM) analysis was made on a Quanta FEG (FEI, the Netherlands) electron microscope at an accelerating voltage of 10 KV. Composite samples were adhered to a conductive carbon tape, and a sputter coated with Au/Pd.

2.9. Statistical analysis

Statistical differences in the film functional properties between samples were analyzed by analysis of variance (ANOVA). Duncan's multiple range test ($p < 0.05$) was adopted to detect differences among mean values of film properties. Statistical analysis was conducted with SPSS 17.0 for windows.

3. Results and discussion

3.1. Effect of clay types on mechanical properties of starch–nanoclay composite films

Mechanical properties of starch–nanoclay composite films included two parts: vertical and horizontal directions. The direction which is consistent with the pulling trend is usually called the vertical direction (Fig. 1), while the direction keeping at a 90° angle with a pulling trend is named the horizontal direction. Fig. 2 indicated the tensile strength (TS, MPa) and elongation at break (*E*, %) of various TPS/clay hybrids containing 6% of clays.

Fig. 2 showed that the addition of various clays to starch improved the tensile strength of the films but lowered the elongation at break. Compared with the contrast film, the tensile strength of starch–clay films showed an increment of 150–310% in Fig. 2a. A similar result was observed by other researchers (Cyras, Manfredi, Minh-Tan, & Vazquez, 2008). Starch-DK3 composite film showed the greatest tensile strength of 2.47 MPa. This suggested that hydroxypropyl distarch phosphate had a good compatibility with DK3 which had a medium hydrophilic property among the clays. All the films showed a good property of elongation at break though it decreased from 150% to 75.8% with the addition of clays in

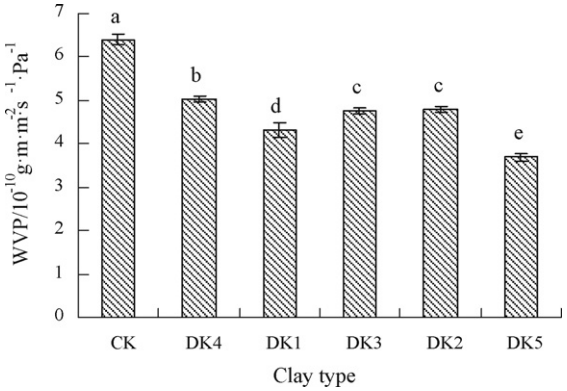

Fig. 3. Water vapor permeability (WVP) of starch–nanoclay composite films (CK – blank control).

Fig. 2b. This was consistent with a previous report which suggested that good dispersion of layers in the polymer reduced tensile ductility and improved strength compared to neat polymer (Lee, Jung, Hong, Rhee, & Advani, 2005). The coupling between the tremendous surface area of the clay and the starch matrix facilitated the stress transfer to the reinforcement phase, allowing for such tensile and toughening improvements (Tang et al., 2008).

Fig. 2 also showed the vertical and horizontal mechanical properties of starch–nanoclay composite films. The tensile strength was lower in the vertical direction whereas elongation at break was higher compared to that of horizontal direction of the films. Contrary to this result, Thunwall et al. (2008) reported that the tensile strength of hydroxypropylated and oxidized potato starch film was higher in the vertical direction than in the horizontal direction. The difference may have been caused by various film blowing conditions. Ghaneh-Fard (1999) studied the effects of blow-up ratio and take-up ratio on molecular orientation and mechanical properties of polyethylene films. The author found that the modulus values decreased with the increase of take-up-ratio in both vertical and horizontal directions for the linear low density polyethylene. But there was a considerable increase for modulus in the horizontal direction as take-up ratio increased at low blow-up ratio. The effects of blowing conditions on the mechanical properties of starch-based films should be further studied.

3.2. Effect of clay types on WVP of starch–nanoclay composite films

Fig. 3 showed the moisture barrier properties of starch–nanoclay composite films. With an addition of 6% clays, the WVP of composite films decreased significantly from 6.40×10^{-10} to 3.69×10^{-10} g m/(m^2 s Pa), which indicated that the layered structure of clay hindered the transmission of moisture vapor through the film matrix (Park et al., 2002). Starch-DK5 composite film had the lowest WVP which suggested the higher hydrophilic property of the clay was, the harder the water molecules went

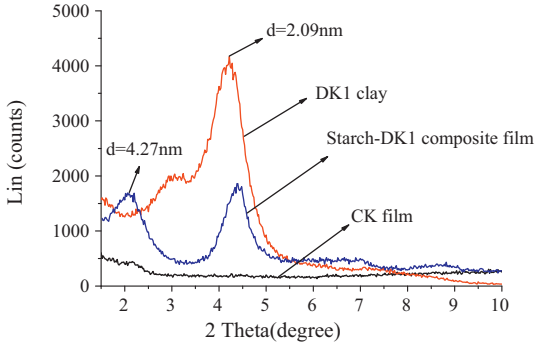

a. XRD patterns of DK1 and composite film

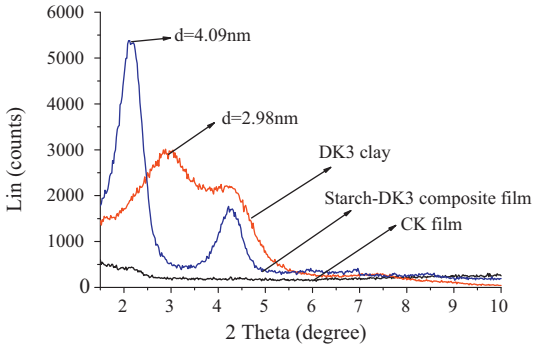

c. XRD patterns of DK3 and composite film

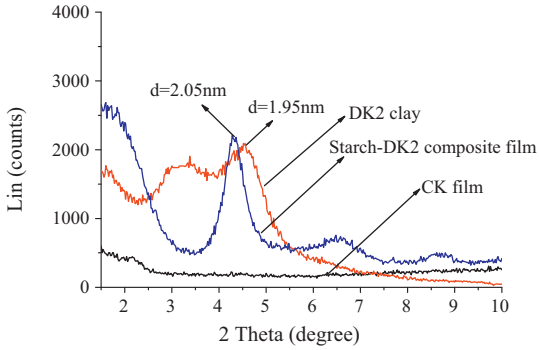

b. XRD patterns of DK2 and composite film

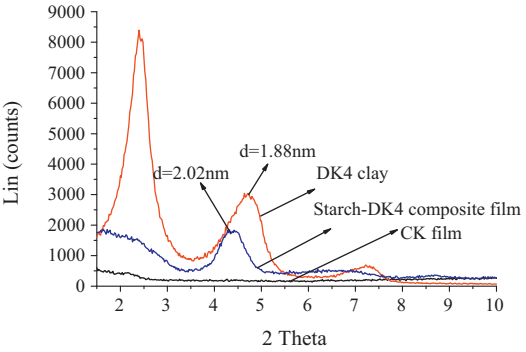

d. XRD patterns of DK4 and composite film

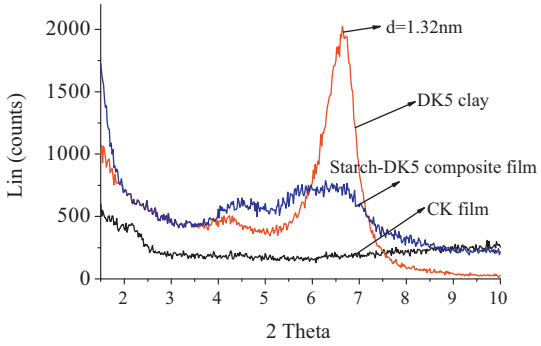

e. XRD patterns of DK5 and composite film

Fig. 4. XRD patterns of films with different nanoclay types (CK – blank control).

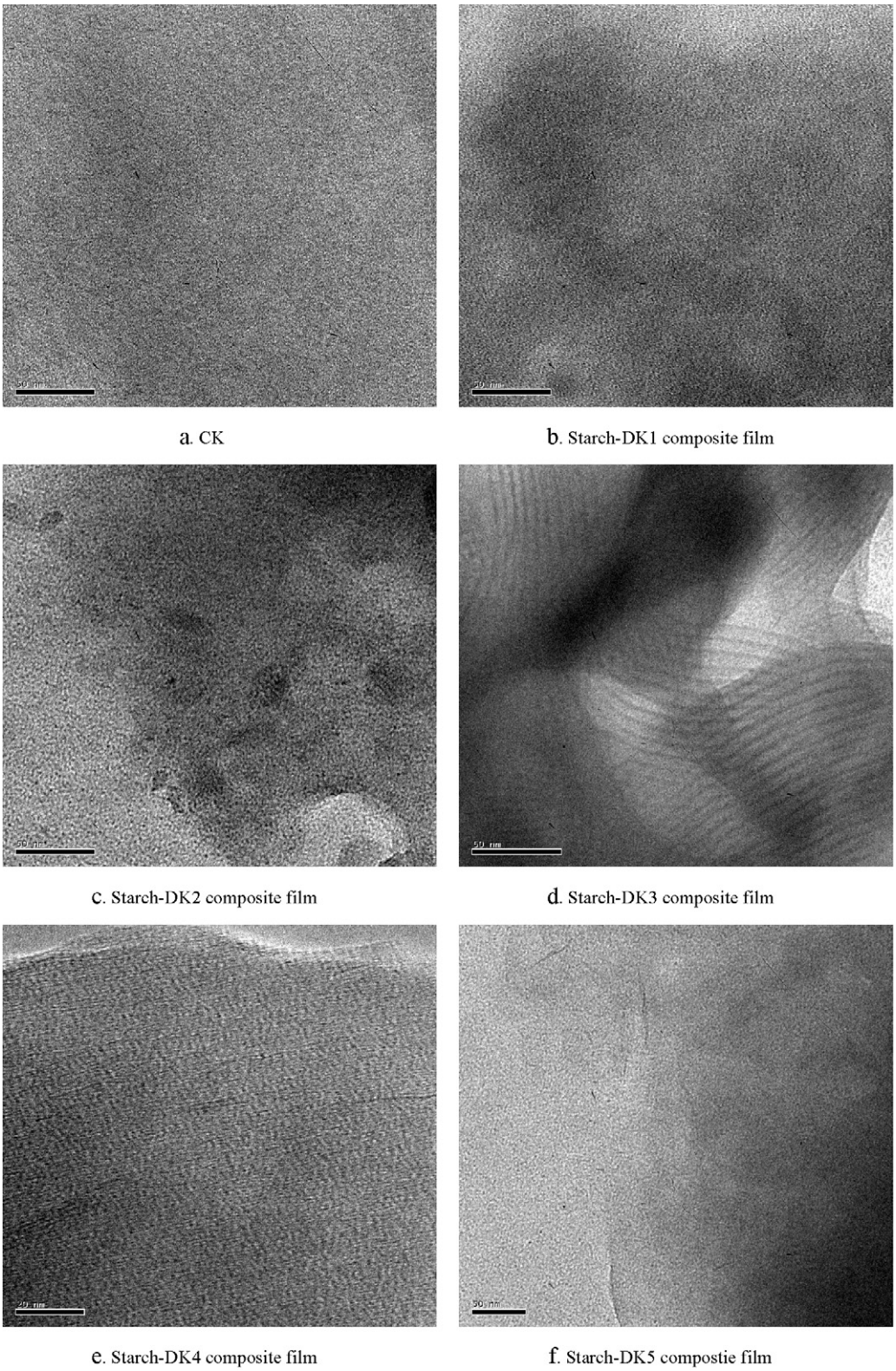

Fig. 5. TEM micrographs of the films with different nanoclay types (CK – blank control).

through the films. Generally, water vapor transmission through a hydrophilic film depends on both diffusivity and solubility of water molecules in the film matrix. When the nanocomposite structure formed, the impermeable clay layers mandated a tortuous pathway for water molecules to traverse the film matrix, thereby increasing the effective path length for diffusion (Tang et al., 2008).

Another factor responsible for the moisture barrier property of starch–clay nanocomposites was the strong molecular interaction between starch molecules and clays with a large surface area (Gusev & Lusti, 2001). The dispersion of clays with various hydrophilicities in starch matrix resulted in different interactions between starch matrix and clays. DK5 may have a stronger

Table 1
The effect of clay types on thermal properties of starch–nanoclay composite films.

Specimens	T_g (°C)	T_o (°C)	T_p (°C)	Rang of ($T_p - T_o$) (°C)
CK-film	9.3	136.9	177.1	40.2
DK4-film	10.3	136.3	168.1	31.8
DK1-film	−7.2	122	163.3	41.3
DK3-film	−23.8	67.5	111.8	44.3
DK2-film	−12.7	125.8	169.6	43.8
DK5-film	−12.9	133.2	173.5	40.3

interaction with starch matrix which caused large amounts of immobile starch molecules and thus lowered moisture permeability.

The value of WVP was greater for the film without clay as the films held substantial amounts of water within the starch–plasticizer network. The absorbed moisture, due to plasticization, had a swelling effect that tended to increase the film permeability to water vapor. Swelling also disrupted the structural integrity and barrier properties of the polymer network (Pushpadass, Marx, Wehling, & Hanna, 2009).

3.3. Effect of clay types on thermal properties of starch–nanoclay composite films

Differential scanning calorimetry (DSC) is a common technology for the determination of transition temperatures. The T_g, T_o and T_p of the starch–clay composite films were presented in Table 1. With increased hydrophilic property of the clays, T_g reduced at the beginning and then went up. The range between T_o and T_p of starch films became wide and then narrow which indicated the clay with medium hydrophilic property had a greater effect on transition temperatures of the films. With the addition of clays, the intermolecular attraction of thermoplastic starch matrix seemed to be interrupted by the charged clays. And subsequently the film backbone chains gained additional segmental mobility which led to the decrease of T_g (Lee et al., 2003). The higher content of modifier (data was not provided) in clays in free and/or combined form would be another factor which reduced the T_g of starch–clay nanocomposite films.

Thermal transition temperatures are typically used to determine the sealing temperatures of polymers (Hernandez, 1997). Table 1 showed the T_o and T_p of the starch–nanoclay composite films and those of the contrast film. The starch-DK3 composite film had the lowest onset temperature and the range between the peak temperature and the onset temperature of starch-DK3 composite film was wider than that of other films. In other words, if all the starch–clay films were heated from their onset temperature, starch-DK3 composite film would finally melt, congeal and lose its structure. The starch-DK3 composite film had a better heat endurance due to the significant difference between T_o and T_p, which is important in good sealing (Abdorreza, Cheng, & Karim, 2011). If the T_o and T_p values were very close, the film would almost completely melt and lose its structure in sealing (Tanner, Getz, Burnett, Youngblood, & Draper, 2003).

3.4. Effect of clay types on structure characteristics of starch–nanoclay composite films

The XRD could provide useful information on the intercalation and exfoliation processes in clay–polymer composites. During the intercalation process the polymer molecules entered the clay galleries and forced apart layers, thus increasing the *d*-spacing (McGlashan & Halley, 2003). This would cause a shift of the diffraction peak to a lower angle. As more polymers entered the gallery, the layers became disordered and some layers were even pushed apart from the stacks of clay particles (partial exfoliated). This would cause XRD peaks with a wider distribution or even a further shift to the left side.

Fig. 4 showed the XRD patterns of the films with different nanoclay types. The dispersion states of nanoclays in the starch matrix depended on the type of clay used. Starch film without clay exhibited a featureless curve in the range of 1–10° (Fig. 4a–e). DK1 exhibited a peak at $2\theta = 4.22°$ ($d = 2.09$ nm), whereas the starch/DK1 composite film showed a new peak at $2\theta = 2.07°$ ($d = 4.27$ nm) (Fig. 4a), and the feature peak of DK1 became weak. It indicated that starch molecules had entered the clay galleries, but incompletely. DK2 exhibited a prominent peak at $2\theta = 4.54°$ ($d = 1.95$ nm), while the starch/DK2 film showed a new peak at $2\theta = 4.32°$ ($d = 2.05$ nm) (Fig. 4b). It suggested that the starch had a weak interaction with DK2. DK4 also had weak interaction with starch (Fig. 4d). It can be seen from Fig. 4c that starch entered DK3 galleries completely, with the dominating peak angle shifting from 2.96° ($d = 2.98$ nm) to 2.15° ($d = 4.09$ nm), indicating the formation of intercalation compounds. DK5 exhibited a sharp peak at 6.67° ($d = 1.32$ nm) while starch-DK5 film showed weak peak just under the original peak of DK5 (Fig. 4e). It suggested that the DK5 could be almost totally exfoliated in the starch matrix. Although the phenomenon of exfoliation was desirable for the improvement of mechanical properties (Wilhelm et al., 2003a, 2003b), the TS of starch-DK5 film was not the biggest one. The organically modified clays and/or their starch-based nanocomposites in this study had two XRD peaks which suggested that new orderly composite structures were formed between clay and modifiers or starch molecules. The forming mechanism of new orderly composite structure should be further studied. The above results clearly showed that DK3 which had a medium hydrophilic property could more easily form intercalation nanocomposite with HPDSP. Water and glycerol content can also change the clay peak positions in X-ray diffraction patterns according to the report of Wilhelm et al. (2003a, 2003b). So their content was invariable for all the films in the whole preparation and testing process.

TEM images provided further evidence for the occurrence of intercalation and exfoliation processes. TEM allowed a qualitative understanding of the internal structure, spatial distribution and dispersion of nanoparticles within the polymer matrix through direct visualization (Tang et al., 2008). TEM micrographs of the films with different types of nanoclays were presented in Fig. 5. The TEM results corresponded well with the XRD patterns. Starch–DK3 composite film exhibited a multilayered nanostructure (Fig. 5d), whereas other starch–clay composite films showed less and even no intercalated multilayered morphology. Instead, they had tactoids (Fig. 5c) or individual layers (Fig. 5b, e and f).

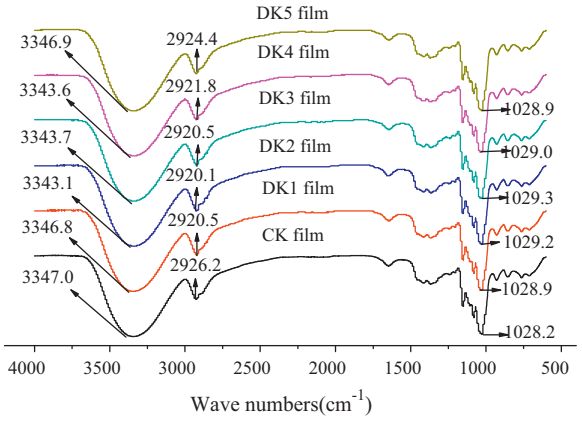

Fig. 6. FT-IR spectra of starch–nanoclay composite films (CK – blank control).

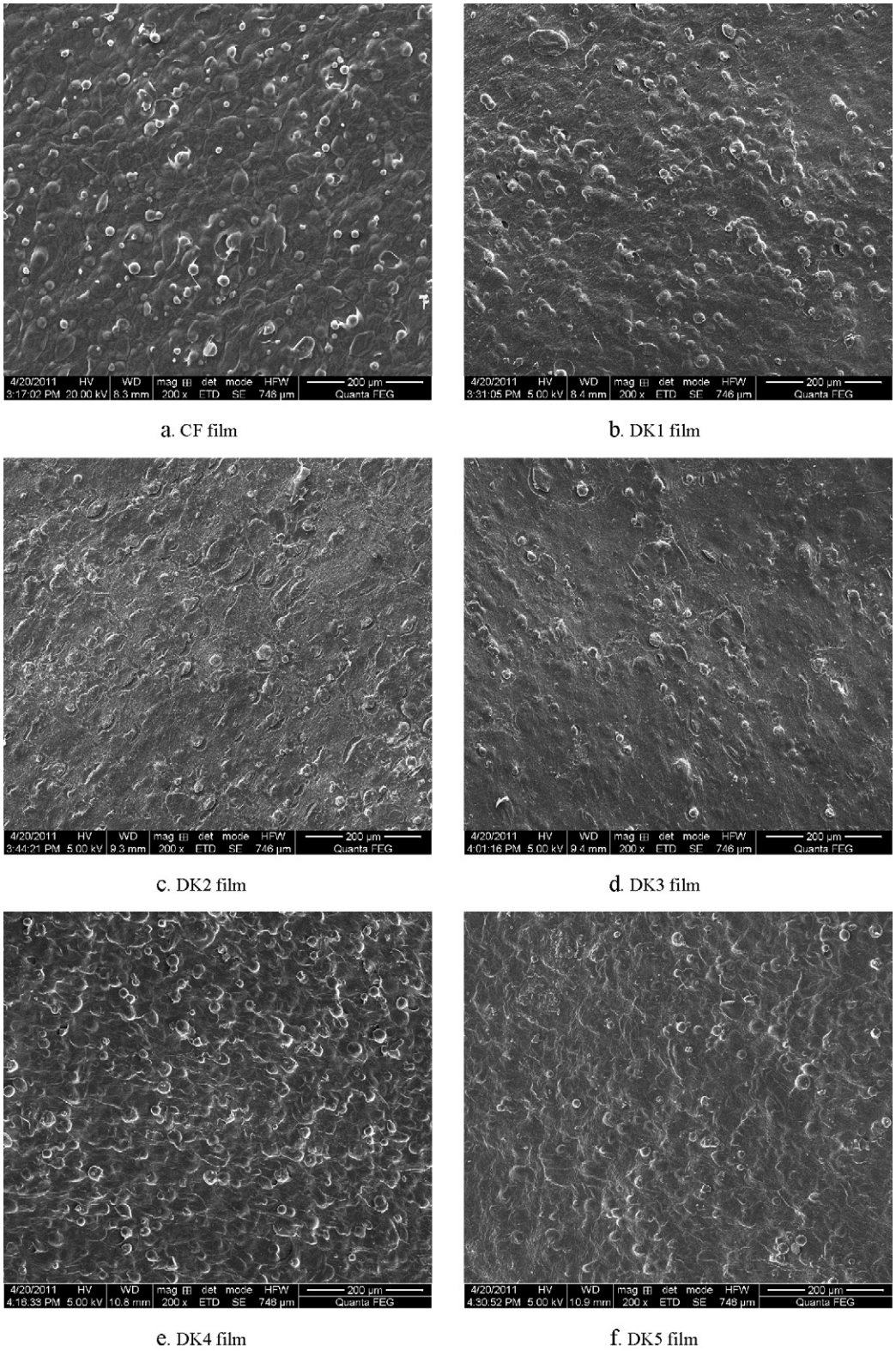

Fig. 7. SEM micrographs of starch–nanoclay composite films (CK – blank control).

3.5. *Effect of clay types on hydrogen bonding interaction of starch–nanoclay composite films*

FTIR analysis is a useful tool to analyze the interactions between starch molecules and plasticizers or clays. According to the harmonic oscillator model, the peak frequency reduced with the increase of the molecular interaction (Pawlak & Mucha, 2003). Fig. 6 showed the FTIR spectra of starch–nanoclay composite films and that of the contrast film.

Zullo and Iannace (2009) thought the peaks in 3340 and 2929 cm^{-1} were associated with inter- and intra-molecular interaction that did not take part in the thermoplasticization. It was

observed from Fig. 6 that the peak at 3347.0 and 2926.2 cm^{-1} of the contrast film was reduced to 3343.1 and 2920.1 cm^{-1} of composite films with clays. Based on the reduction extent of peak frequency near the frequency of 3347 cm^{-1}, DK2, DK3 and DK4 had a stronger interaction with starch molecules than DK1 and DK5. Fig. 6 also showed three significant peaks between 990 and 1200 cm^{-1} which can be attributed to C—O bond stretching. They can be used to evaluate the thermoplasticization process with different types of clays (Fang, Fowler, Tomkinson, & Hill, 2002; Zullo & Iannace, 2009). The peaks at 1028.2, 1081.2 and 1152.6 cm^{-1} of contrast film were shifted to 1029.3, 1081.3 and 1152.9 cm^{-1} indicating that clays inhibited the plastication between starch and glycerol to some extent. In contrast, some of glycerol molecules were intercalated between the layers of the clays (Wilhelm et al., 2003a, 2003b). It was in conformity with the report that the lower the peak frequency of C—O group in starch was, the stronger the interaction was between starch and plasticizers (Ma, Yu, & Wan, 2006).

3.6. Effect of clay types on microstructure of starch–nanoclay composite films

Under the strong shear and high temperature conditions, native starch granules with the action of plasticizer were molten or physically broken up into small fragments. A continuous phase was formed under shear and pressure as a result (Ma et al., 2006). Fig. 7 showed the microstructure of starch–nanoclay composite films and the contrast one. It could be seen from Fig. 7c, d and f that the amount of intact starch granules reduced and the films showed continuous texture. The surfaces of the starch/DK2, DK3, DK5 films were smooth while the starch/DK1, DK4 films were rough. This indicated that DK2, DK3 and DK5 were compatible with starch matrix. DK1 and DK4 clays seemed to have little effect on the continuity of films compared to control film (Fig. 7b and e). In contrast to other films, starch–DK3 film (Fig. 7d) had a more homogeneous phase. It turned out that DK3 which had a medium hydrophilic property was more efficient in starch granules, melting and fracturing than other clays due to its good compatibility with HPDSP.

4. Conclusion

The hydrophilicities of clays had significant effects on properties of starch–nanoclay composite films. The starch–clay composite films showed higher tensile strength and better barrier properties to water vapor than the contrast film. The starch–clay films had a lower glass transition temperature (T_g) and better heat endurance compared to the contrast film. The microstructure of the films was more homogeneous and smooth with the addition of clays into starch. The clay which had a medium hydrophilic property was more suitable for the preparation of hydroxypropyl distarch phosphate–clay nanocomposite films as an intensifier among all the five clays.

Acknowledgements

The financial support from National High-tech Research and Development Program of China (2007AA100407) and Department of Science and Technology of Shandong Province (2010GNC10927) is greatly acknowledged.

References

Abdorreza, M. N., Cheng, L. H., & Karim, A. A. (2011). Effects of plasticizers on thermal properties and heat sealability of sago starch films. *Food Hydrocolloids*, *25*, 56–60.
ASTM. (2002). Standard test method for tensile properties of thin plastic sheeting, D882-02. In *Annual Book of ASTM Standards*. Philadelphia, PA: American Society for Testing and Material.
Avella, M., De Vlieger, J. J., Errico, M. E., Fischer, S., Vacca, P., & Volpe, M. G. (2005). Biodegradable starch/clay nanocomposite films for food packaging applications. *Food Chemistry*, *93*, 467–474.
Azeredo, H. M. C. de. (2009). Nanocomposites for food packaging applications. *Food Research International*, *42*, 1240–1253.
Carvalho, D. A. J. F., Curvelo, A. A. S., & Agnelli, J. A. M. (2001). A first insight on composites of thermoplastic starch and Kaolin. *Carbohydrate Polymers*, *45*, 189–194.
Chen, B. q., & Evans, J. R. G. (2005). Thermoplastic starch–clay nanocomposites and their characteristics. *Carbohydrate Polymers*, *6*, 455–463.
Chiou, B. S., Wood, D., Yee, E., Imam, S. H., Glenn, G. M., & Orts, W. J. (2007). Extruded starch–nanoclay nancomposites: Effects of glycerol and nanoclay concentration. *Polymer Engineering Science*, *47*, 1898–1904.
Chung, Y. L., Ansari, S., Estevez, L., Hayrapetyan, S., Giannelis, E. P., & Lai, H. M. (2010). Preparation and properties of biodegradable starch–clay nanocomposites. *Carbohydrate Polymers*, *79*, 391–396.
Cyras, V. P., Manfredi, L. B., Minh-Tan, T.-T., & Vazquez, A. (2008). Physical and mechanical properties of thermoplastic starch/montmorillonite nanocomposite films. *Carbohydrate Polymers*, *73*, 55–63.
Fang, J. M., Fowler, P. A., Tomkinson, J., & Hill, C. A. S. (2002). The preparatianion and characterisation of a series of chemically modified potato starches. *Carbohydrate Polymers*, *47*(3), 245–252.
Ghaneh-Fard, A. (1999). Effects of film blowing conditions on molecular orientation and mechanical properties of polyethylene films. *Journal of Plastic Film and Sheeting*, *15*(3), 194–218.
Guan, J. j., Eskridge, K. M., & Hanna, M. A. (2005). Acetylated starch–polylactic acid loose-fill packaging materials. *Industrial Crops and Products*, *22*, 109–123.
Gusev, A. A., & Lusti, H. R. (2001). Rational design of nanocomposites for barrier applications. *Advanced Materials*, *13*(21), 1641–1643.
Hernandez, R. J. (1997). Polymer properties. In A. L. Brody, & K. Marsh (Eds.), *The Wiley encyclopedia of packaging technology* (2nd ed, pp. 758–765). New York: John Wiley and Sons Inc.
Huang, M., Yu, J. G., & Ma, X. F. (2006). High mechanical performance MMT-urea and formamide-plasticized thermoplastic cornstarch biodegradable nanocomposites. *Carbohydrate Polymers*, *63*, 393–399.
Kalambur, S. B., & Rizvi, S. S. H. (2004). Starch-based nanocomposites by reactive extrusion processing. *Polymer International*, *53*, 1413–1416.
Lee, J. H., Jung, D., Hong, C. E., Rhee, K. Y., & Advani, S. G. (2005). Properties of polyethylene-layered silicate nanocomposites prepared by melt intercalation with a PP-g-MA compatibilizer. *Composites Science and Technology*, *65*, 1996–2002.
Lee, J. H., Park, T. G., Park, H. S., Lee, D. S., Lee, Y. K., Yoon, S. C., et al. (2003). Thermal and mechanical characteristics of poly(1-lactic acid) nanocomposite scaffold. *Biomaterials*, *24*, 2773–2778.
Lopez, O. V., Garcıa, M. A., & Zaritzky, N. E. (2008). Film forming capacity of chemically modified corn starches. *Carbohydrate Polymers*, *73*, 573–581.
Ma, X. F., Yu, J. G., & Wan, J. J. (2006). Urea and ethanolamine as a mixed plasticizer for thermoplastic starch. *Carbohydrate Polymers*, *64*, 267–273.
McGlashan, S. A., & Halley, P. J. (2003). Preparation and characterization of biodegradable starch-based nanocomposite materials. *Polymer International*, *52*, 1767–1773.
Medeiros, E. S., Dufresne, A., & Orts, W. J. (2010). Starch-based nanocomposites. In A. C. Bertolini (Ed.), *Starch: Characterization, properties, and applications* (pp. 250–252). Boca Raton: Taylor and Francis Group, LLC.
Park, H., Li, X., Jin, C., Park, C., Cho, W., & Ha, C. (2002). Preparation and properties of biodegradable thermoplastic starch/clay hybrids. *Macromolecular Material and Engineering*, *287*, 553–558.
Pawlak, A., & Mucha, M. (2003). Thermogravimetric and FTIR studies of chitosan blends. *Thermochimica Acta*, *396*(1–2), 153–166.
Pushpadass, H. A., Marx, D. B., Wehling, R. L., & Hanna, M. A. (2009). Extrusion and characterization of starch films. *Cereal Chemistry*, *86*(1), 44–51.
Qiao, X. y., Jiang, W. b., & Sun, K. (2005). Reinforced thermoplastic acetylated starch with layered silicates. *Starch/Starke*, *57*, 581–586.
Sarazin, P., Li, G., Orts, W. J., & Favis, B. D. (2008). Binary and ternary blends of polylactide, polycaprolactone and thermoplastic starch. *Polymer*, *49*, 599–609.
Siracusa, V., Rocculi, P., Romani, S., & Rosa, M. D. (2008). Biodegradable polymers for food packaging: A review. *Trends in Food Science and Technology*, *19*, 634–643.
Sita, C., Burns, M., Haßler, R., & Focke, W. W. (2006). Tensile properties of thermoplastic starch–PVB blends. *Journal of Applied Polymer Science*, *101*, 1751–1755.
Sudhamani, S. R., Prasad, M. S., & Udaya Sankar, K. (2003). DSC and FTIR studies on Gellan and polyvinyl alcohol (PVA) blend films. *Food Hydrocolloids*, *17*, 245–250.
Tang, X. Z., Alavi, S., & Herald, T. J. (2008). Barrier and mechanical properties of starch–clay nanocomposite films. *Cereal Chemistry*, *85*(3), 433–439.
Tanner, K. E., Getz, J. J., Burnett, S., Youngblood, E., & Draper, P. R. (2003). Film forming compositions comprising modified starches and iota-carrageenan and methods for manufacturing soft capsules using same. *US Patent*, *6*, 582–727.
Thunwall, M., Kuthanova, V., Boldizar, A., & Rigdahl, M. (2008). Film blowing of thermoplastic starch. *Carbohydrate Polymers*, *71*, 583–590.
Wilhelm, H. M., Sierakowski, M. R., Souza, G. P., & Wypych, F. (2003a). Starch films reinforced with mineral clay. *Carbohydrate Polymers*, *52*(2), 101–110.
Wilhelm, H. M., Sierakowski, M. R., Souza, G. P., & Wypych, F. (2003b). The influence of layered compounds on the properties of starch/layered compound composites. *Polymer International*, *52*(6), 1035–1044.
Zullo, R., & Iannace, S. (2009). The effects of different starch sources and plasticizers on film blowing of thermoplastic starch: Correlation among process, elongational properties and macromolecular structure. *Carbohydrate Polymers*, *77*, 376–383.